Journal of Materials Chemistry A

Accepted Manuscript

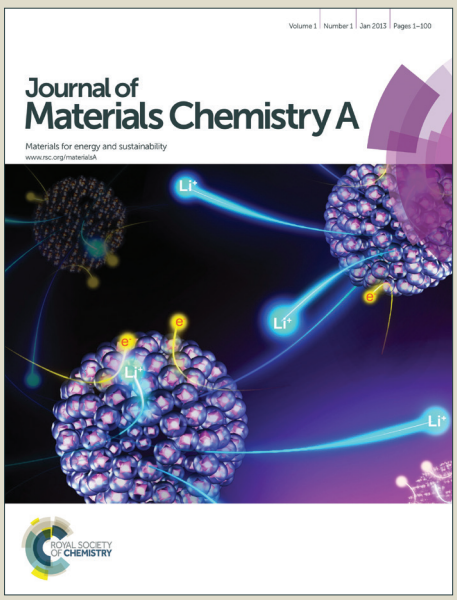

ROYAL SOCIETY OF CHEMISTRY

www.rsc.org/materialsA

Development of Supramolecular Liquid-Crystalline Polyurethane Complexes Exhibiting Triple-shape Functionality Using a One-step Programming Process

Shaojun Chen[1], Hongming Yuan[1], Shiguo Chen[1], Haipeng Yang, Zaochuan Ge[1]*[a)],

Haitao Zhuo[2]*[b)], Jianhong Liu[2],

[1]*Shenzhen Key Laboratory of Special Functional Materials, College of Materials Science and Engineering, Shenzhen University, Shenzhen,518060, China.* [2]*Shenzhen Key Laboratory of Functional Polymer, College of Chemistry and Chemical Engineering, Shenzhen University, Shenzhen, 518060, China.*

*Corresponding author: College of Materials Science and Engineering，Shenzhen University, Shenzhen 518060, China. Tel and Fax: +86-755-26534562. E-mail: [a)]Z.C.Ge gezc@szu.edu.cn; [b)]H.T.Zhuo haitaozhuo@163.com

Electronic Supplementary Information (ESI) available:

Video A*. POM video of HOBA for isotropic phase to smectic C phase transition at 138 °C

Video B*. POM video of SLCSMPU complex for Smectic C phase at 128 °C

Fig. A* Photos of a PySMPU-1.3HOBA sample with a perfect polymeric film

Fig. B* the first DSC heating curves for pure HOBA (a) and SMPU-0.8HOBA (b) showing the main phase transitions

Fig.C* the second DSC heating curves of (a) pure HOBA and (b) SMPU-0.6HOBA showing the crystal melting process and entering mesophic phase process

Fig.D* POM images (×400) of pure HOBA showing the phase transition process

Fig.E* POM images (×400) of SMPU-0.6HOBA showing the phase transition process

Fig.F* Temperature-dependent Frequencies for SMPU and SMPU-0.8HOBA at the position of N-H group (a) and pyridine ring (b)

Fig.G* Triple shape recovery process of sample PySMPU-0.6HOBA

Abstract:

Supramolecular liquid crystalline polymers and shape memory polymers are attracting increasing interest as materials. In this paper, we describe the development of a supramolecular liquid crystalline shape memory polyurethane (SLCSMPU) complex that exhibits both liquid crystalline properties and shape memory properties. The complex is formed by incorporating 4-hexadecyloxybenzoic acid (HOBA) into a pyridine-containing shape memory polyurethane (PySMPU). The HOBA is tethered to the PySMPU by strong hydrogen bonding between the pyridine rings and the COOH of the HOBA, forming a SLCSMPU complex. Heat treatment plays an important role in the formation of hydrogen-bonded supramolecular liquid crystalline structures in these SLCSMPU complexes. Thus, the SLCSMPU complex not only maintains the intrinsic liquid-crystalline properties of HOBA, but can also form a stable polymeric film for various shape memory applications. Additionally, the SLCSMPU complex forms a two-phase separated structure composed of an amorphous polyurethane matrix and a HOBA crystalline phase, which includes the hydrogen-bonded crystalline HOBA phase and the free HOBA crystalline phase. Therefore, a simple one-step programming process is developed that produces SLCSMPU complexes with excited triple-shape functionalities due to their multiple phase transitions, especially when the molar ratio of HOBA/BINA is less than 0.8.

Keywords: shape memory, polyurethane, supramolecular, liquid crystalline;

1. Introduction

Shape memory polymers (SMPs) have attracted significant interest in recent years.[1] Conventional thermal-induced SMPs are dual-SMPs, which can only fix to one temporary shape before converting back to their original shapes when heated to their transition temperatures.[2, 3] In the past decades, a great deal of effort has been made to improve or modify shape memory effects (SMEs).[4] Consequently, triple-SMPs,[5-9] quadruple-SMPs [10] and multiple-SMPs [11, 12] have been developed. In contrast to dual-SMPs, these new types of SMPs can recover their original shapes from more than one temporary shape. That is, triple-SMPs can move from a first shape (A) to a second shape (B) and, from there, to a third shape (C), with increasing temperature.[13, 14] This triple-shape capability is based on a multiphase polymer network structure with at least two phase-separated domains. These domains each have a transition temperature (T_{trans}), which can be a glass transition temperature (T_g), a melting temperature (T_m) or a liquid crystalline transition temperature (T_i). Thus, triple-shape functionality can easily be achieved by polymer blending, laminating and hybridising.[13-15] A two-step programming process is usually required to achieve triple-shape functionality, which allows the stepwise conversion to two independent shapes (A and B).[15] However, a recently developed one-step programming process can facilitate triple-shape technology, while substantially increasing the attractiveness of this technology for technical and medical applications.[16] Therefore, triple-shape functionality generated by one-step programming processes represents a new direction for SMP research.

Supramolecular chemistry has also been widely used in recent years to construct SMPs.[17-22] Supramolecular shape memory materials are synthesised by utilising supramolecular switches or supramolecular net points. For example, Zhang *et al*. reported several supramolecular SMPs based on partial cyclodextrin CD inclusion complexes[19, 21]. These supramolecular complexes were biodegradable and responded to pH, redox reactions and glucose.[23] Additionally, photo-cross-linked metallo-supramolecular polymers also exhibit thermo-, photo-, and chemo-responsive shape memory properties.[17, 22] Moreover, triple-shape functionalities have been achieved in some supramolecular polymer complexes or composites. For example, Ware et al. reported a system based on an acrylic triple-SMP supramolecular complex that utilised the glass transition and dissociation of self-complementary hydrogen bonding moieties.[6] Chen et al. developed a simple and controllable strategy to synthesise a triple-shape memory supramolecular composite using intermolecular hydrogen bonding between a polymer and mesogenic units.[24] These studies suggest that supramolecular polymer systems can be used to simplify and control the production of blocks for triple-shape functionality.

Supramolecular liquid crystalline complexes are important supramolecular systems that are formed by

non-covalent bonding. These complexes have attracted much attention and become good candidates for the next generation of advanced functional materials.[25, 26] In these supramolecular liquid crystalline complexes, the mesogenic properties are tailored *via* non-covalent interactions. Since Kato and colleagues first exploited the H-bonding between carboxylic acids and pyridines to induce liquid crystalline properties, the carboxylic acid-pyridine complex has been widely investigated.[27-29] It has been reported that supramolecular liquid crystalline polyurethane complexes can be easily formed *via* hydrogen bonding between pyridine rings and the carboxylic acids of mesogens such as 4-dodecyloxybenzoic acid, 4-octyloxybenzoic acid and 4-butyloxybenzoic acid.[30, 31] However, to our knowledge, there are few reports about supramolecular liquid crystalline complexes with triple-shape functionality. Recently, we reported supramolecular shape memory polyurethanes containing pyridine moieties (PySMPUs), [22, 32-35] which exhibit not only thermal-induced shape memory effects[22] but also moisture-sensitive shape memory effects.[33] Thus, it is desirable to further develop supramolecular liquid crystalline shape memory polyurethanes (SLCSMPUs) that have both liquid crystalline properties and shape memory properties by modifying the PySMPUs with mesogens based on p-n-alkoxybenzoic acids. [30, 31, 36]

In our earlier communication, we prepared liquid crystalline shape memory polyurethane composites with both liquid crystalline properties and shape memory properties using polymer bending of shape memory polyurethane with an amorphous reversible phase and 4-hexadecyloxybenzoic acids (HOBA).[37] Inspired by this pioneering work, we now propose another type of SLCSMPU complex for triple-shape applications. In this new complex, PySMPU, which contains many pendent pyridine rings that serve as H-acceptors, is first prepared with N,N-bis(2-hydroxylethyl)isonicotinamine (BINA) and 1,6-hexanediisocyante (HDI).[38] SLCSMPU complexes are then prepared by incorporating HOBA within the PySMPUs in a DMF solution. The SLCSMPU complexes are then obtained after drying the PySMPU-HOBA mixtures. In contrast to the previous triple-SMPs produced through a two-step programming process, these complexes achieve triple-shape functionality with a simple one-step programming process followed by staged heating recovery conditions. We report the structure, morphology, liquid crystalline properties, and, particularly, the triple-shape memory properties of these SLCSMPU complexes.

2. Experimental

2.1 Synthesis of the PySMPUs

BINA was purchased from Jiaxing Carry Bio-Chem Technology Co. Ltd. HDI and Dimethylformamide (DMF, HPLC) were purchased from Aladdin-reagent (Shanghai) Co. Ltd. The PySMPUs were prepared with BINA and HDI in the 10wt% DMF solution at a 1:1.05 molar ratio of OH to NCO according to the synthesis procedure

described previously[22]. The synthesis routine is presented in **Scheme 1**. The reaction was carried out in a 500 mL flask filled with nitrogen and equipped with a mechanical stirrer, a thermometer, and a condenser. First, the BINA powder and DMF were added to the flask. After dissolving the BINA powder through mechanical stirring, an equimolar amount of HDI was added to the flask. The oil temperature was then raised to 80 °C, before 0.02 wt% dibutyltin dilaurate catalyst was added to the reaction. During the reaction, 10 mL volumes of DMF each time were occasionally added to the reaction to keep a suitable viscosity (about 40mpa.s at 80 °C) of the solution. The reaction was maintained for 4 hours to obtain the 10 wt% PySMPU/DMF solution.

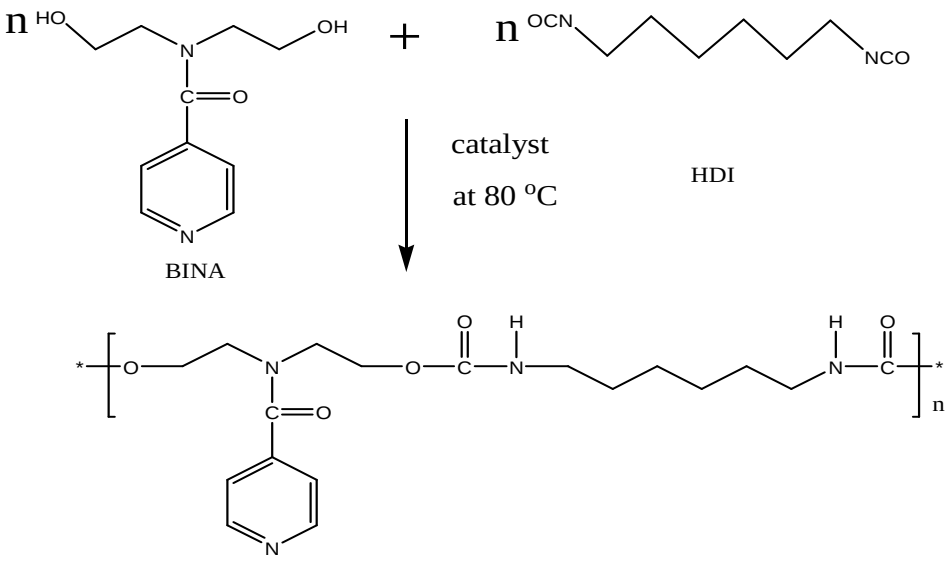

Scheme 1. Synthesis of PySMPU based on BINA and HDI

2.2 Preparation of the SLCSMPU Complexes

Table 1. Composition of SLCSMPU complexes based on PySMPU and HOBA

Samples	PySMPU (g)	HOBA (g)	HOBA content (wt%)	Molar ratio of HOBA/BINA
Pure PySMPU	10.0	--	--	--
PySMPU-0.2HOBA	10.0	1.68	14.4	0.2
PySMPU-0.4HOBA	10.0	3.36	25.1	0.4
PySMPU-0.6HOBA	10.0	5.04	33.5	0.6
PySMPU-0.8HOBA	10.0	6.72	40.2	0.8
PySMPU-1.0HOBA	10.0	8.40	45.7	1.0
PySMPU-1.3HOBA	10.0	10.92	52.2	1.3

According to the composition of the SLCSMPU complex listed in Table 1, a certain quantity of HOBA, e.g., 1.68 g, was added to the 10wt% PySMPU/DMF solution containing approximately 10.0 g of PySMPU resin. Under strong mechanical stirring, the PySMPU and the HOBA were mixed for 2 hours to obtain a homogenous solution-phase mixture. Finally, the SLCSMPU complexes were obtained by casting the mixture onto a Teflon pan, which was placed at 80 ºC for 24 hours and further dried at 80 ºC under a vacuum of 0.1-0.2 kPa for 24 hours. The samples were coded as PySMPU-#HOBA, with # representing the molar ratio of HOBA/BINA, e.g., sample PySMPU-0.4HOBA.

2.3 Structural Characterisation

FT-IR spectra were obtained from smooth 0.2 mm-thick polymer films using a Nicolet 760 FT-IR spectrometer and the FT-IR attenuated total reflection (ATR) method. Ten scans at 4 cm^{-1} resolution were averaged and stored as data files for further analysis.

DSC curves were obtained using a TA Q200 instrument with nitrogen as a purge gas. Indium and zinc standards were used for calibration. The samples were first heated from -60 ºC to 200 ºC at a rate of 10 ºC/min. They were then held at 200 ºC for 1 min and cooled to -60 ºC at a rate of 10 ºC/min. Finally, a second heating scan was performed from -60 °C to 200 °C.

Wide angle X-ray diffraction (WAXD) measurements were obtained using a D8 Advance (Bruker, Germany) instrument with an X-ray wavelength of 0.154 nm at a scanning rate of 12°/min. Specimens 0.5 mm thick were prepared for these measurements.

The mesophases were identified and the phase transition temperatures were determined using a Zeiss-Axioscope polarised optical microscopy (POM) equipped with a Linkam-THMS-600 variable-temperature stage at a scan rate of 2 °C/min. The samples were heated from 20 °C to 160 °C and cooled from 160 °C to 20 °C.

The specimens for DMA testing were prepared by casting a 0.5 mm-thick film with a width of 5 mm and a length of 25 mm. The dynamic mechanical properties of the samples were determined using a PerkinElmer DMA at 1 Hz with a heating rate of 2 °C/min from -60 to 130 ºC.

The morphology of the samples was examined using scanning electron microscopy (SEM, Hitachi, Japan). Prior to scanning, the samples were coated with a thin layer of gold.

2.4 The One-step Programming Process for Triple-shape Functionality Characterisation

The triple-shape memory cycles produced using a one-step programming process and staged heating recovery conditions were investigated using a TA Instruments DMA Q800 (tension clamp, controlled force mode). The

samples were dried completely at 100 ºC under vacuum for 24 h. The films were then cut into rectangular specimens 10 mm long, 4.8 mm wide and 0.4 mm thick. The test procedure is shown in Scheme 2. This procedure is similar to the procedure described in the literature.[39] Typically, the process occurs as follows: (1) the rectangular sample is heated and held at 80 ºC for 10 min; (2) the sample is uniaxially elongated by a ramping force from 0.00 N to 0.175 N at a rate of 0.05 N/min and kept fully stretched at a fixed strain; (3) the sample is cooled quickly at a rate of 30 ºC/min to a low temperature at a fixed strain; (4) unloading of the extra force from 0.175 N to 0 N is performed at a rate of 0.05 N/min; (5) on the first heating stage, the sample is reheated to 80 ºC at a rate of 10 ºC/min and held at 80 ºC for 40 min; and (5) on the second heating stage, the sample is reheated to 100 ºC at a rate of 10 ºC/min and held at 100 ºC for another 40 min. During this process, DMA curves showing the strain, temperature and time were recorded for future analysis.

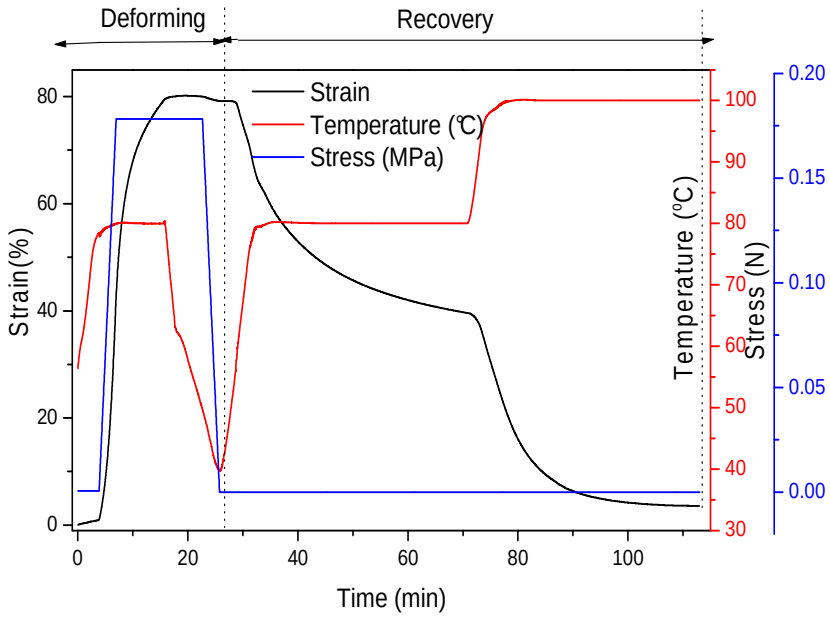

Scheme 2. Triple-shape memory cycle in the one-step programming process and the staged heating recovery conditions

3. Results and Discussion

3.1 Structural analysis

Figure 1(A) shows the FT-IR spectra for PySMPU-0.8HOBA compared with pure PySMPU and pure HOBA. On the basis of our previous FT-IR studies with polyurethane based on BINA, the frequency at 1624 cm^{-1} belongs to the stretching vibration of the C=O beside the pyridine ring of the BINA unit. The frequencies at 1600 cm^{-1}, 1464 cm^{-1}, 1433 cm^{-1}, 1408 cm^{-1}, 1136 cm^{-1}, 1089 cm^{-1}, and 1040 cm^{-1} result from the stretching vibration of the pyridine ring.[40] When HOBA is incorporated into the PySMPU to form the SLCSMPU

complexes, the FT-IR spectra of the PySMPU-0.8HOBA show no obvious frequencies at 1624 cm^{-1} and 1600 cm^{-1}. This implies that the stretching vibration of the BINA unit is limited by the HOBA unit. Additionally, the stretching frequencies of the pyridine ring at 1464 cm^{-1}, 1433 cm^{-1} and 1408 cm^{-1} disappear in the PySMPU-0.8HOBA spectra, while new frequencies appear at 1673 cm^{-1} and 1429 cm^{-1}, which belong to the stretching vibration frequencies of C=O and CH_2 from the HOBA, respectively. This indicates that there should be strong intermolecular forces between the pyridine rings within the HOBA that limit the stretching vibration of the pyridine ring. Figure 1 shows that the broad frequency of HOBA between 1673 and 1693 cm^{-1} tends to be divided into two peaks. The frequency at 1693 cm^{-1} is due to the strengthening of the hydrogen-bonded C=O stretching vibration[30]. This indicates that the original HOBA dimer, which is formed by hydrogen bonding between COOH groups [41], becomes dissociated by participation in another hydrogen-bonded complex. Thus, it can be confirmed that stronger hydrogen bonding occurs between the pyridine rings of PySMPU and the COOH of HOBA in the SLCSMPU complexes. That is, HOBA is tethered to PySMPU as a side chain *via* strong hydrogen bonding. This hypothesis is further confirmed by the FT-IR spectra of the SLCSMPU complexes with different HOBA contents shown in Figure 1(B). The O-H stretching vibration frequency at 3500 cm^{-1} and the benzene ring absorption frequency at 1578 cm^{-1} become more obvious as the HOBA content increases in the SLCSMPU complexes. The frequency at 1624 cm^{-1} can be detected both in the PySMPU-0.2HOBA samples and in the pure PySMPU. However, this frequency disappears when the molar ratio of HOBA/BINA is greater than 0.6. These results give proof for the formation of the supramolecular complexes and suggest that part of the pyridine ring becomes tethered to the HOBA when the molar ratio of HOBA/BINA is below 0.4. In contrast, a lot of free HOBA dimers are maintained in the SLCSMPU complexes at higher HOBA contents. These results are very consistent with the formation of p-n-alkoxy benzoic acid/PySMPU as reported in literatures [31, 36]

According to the above analysis, the possible supramolecular structure of the SLCSMPU complex is shown in Scheme 3. In this study, HOBA molecules with long alkyl chains were selected because they have been reported to only have a reversible smectic C liquid crystalline phase[42-44.] The polyurethane backbone chain composed of HDI and the BINA unit and the pedant pyridine ring were used as H-acceptors.[40] Thus, strong hydrogen bonds were formed between the pyridine rings and the carboxyl groups of HOBA when the PySMPUs based on the HDI-BINA system were mixed with the HOBA to form the PySMPU-HOBA complex. The supramolecular structure of the SLCSMPU complex can be further confirmed by WAXD, as shown in Figure 2. The pure PySMPU had an amorphous phase, while the pure HOBA formed crystals, as indicated by its many crystalline peaks. In the SLCSMPU complexes, e.g., the PySMPU-0.4HOBA and PySMPU-0.4HOBA samples,

almost all of the crystalline peaks for HOBA could be detected. Compared with the pure HOBA, the majority of crystalline peaks shifted to higher 2θ values. This implies that the crystal face distance (*d*) of HOBA becomes smaller in the SLCSMPU complex. In other words, the formation of HOBA crystals is greatly influenced by the PySMPU matrix, possibly because of the formation of strong hydrogen bonds between the PySMPU and HOBA. Thus, we can confirm again that the HOBA is tethered to the PySMPU to form a SLCSMPU complex. In contrast to the previously reported SMPU-LC composites based on SMPU with an amorphous reversible phase,[37] this SLCSMPU complex improves the miscibility between the PySMPU and HOBA. Thus, a large amount of HOBA (up to 52.2 wt% for PySMPU-1.3HOBA) can be added to the PySMPU polymer matrix to form a stable polymer film (see ESI Fig. A†). In a previous report, Chen et al. demonstrated that the liquid-crystalline mesophase was lost when LC mesogens containing pyridine moieties were attached to the SMPU-containing carboxyl groups through hydrogen bonding between the pyridines and the COOH groups.[13] However, in our SLCSMPU complex, the pendant pyridine rings incorporate as side chains on the mesogens. As a result, the intrinsic liquid crystalline properties of HOBA are maintained. The supramolecular liquid crystalline behaviour of the hydrogen-bonded complexes of the non-mesogenic anil with p-n-alkoxybenzoic acid has been investigated systematically in a previous study; and it was reported that the pure HOBA shows only smectic C within the temperature range of 85℃ to 132.5℃.[42] In our study, the formation of SLCSMPU complexes suggests that better liquid crystalline properties can be achieved by adding high amounts of HOBA mesogens. Thus, the SLCSMPU complex polymer film has potential applications in optical devices and sensors, which will be explored in future studies.

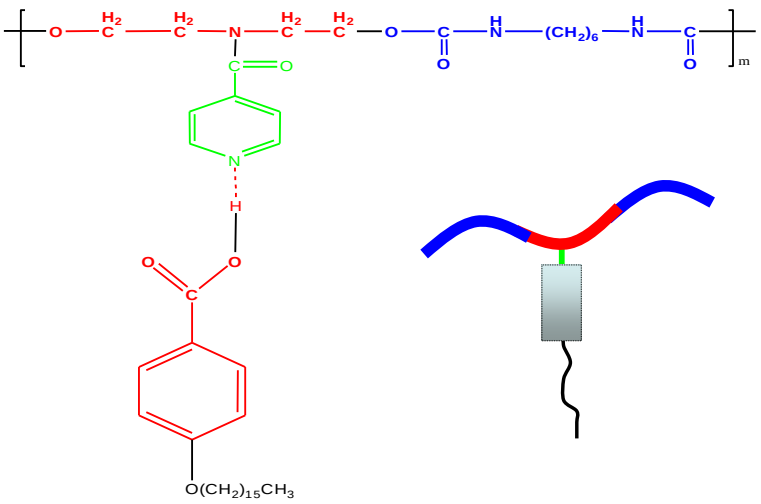

Scheme 3. Supramolecular molecular structure of the SLCSMPU complex

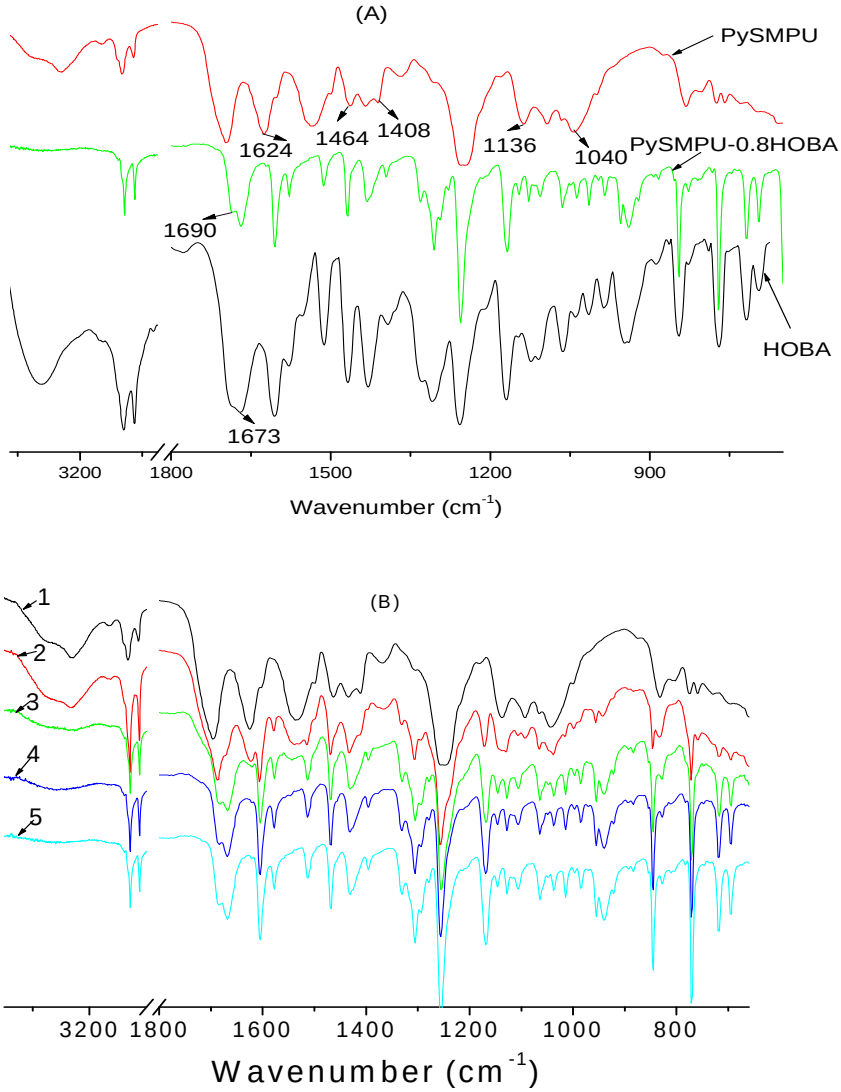

Figure 1. (A) FT-IR spectra for PySMPU-0.8HOBA compared with pure PySMPU and HOBA and (B) FT-IR spectra for SLCSMPU complexes with different HOBA contents (1- PySMPU; 2-PySMPU-0.2HOBA; 3-PySMPU-0.4HOBA; 4-PySMPU-0.6HOBA; 5-PySMPU-0.8HOBA)

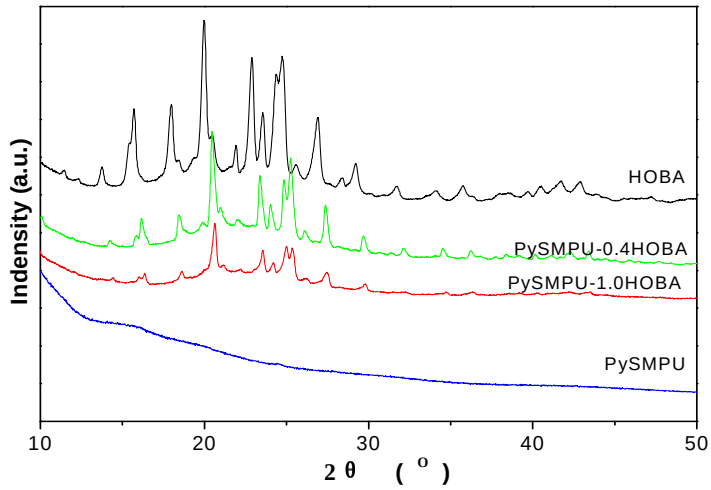

Figure 2. XRD patterns of the SLCSMPU complexes at 25℃

3.2 Thermal properties

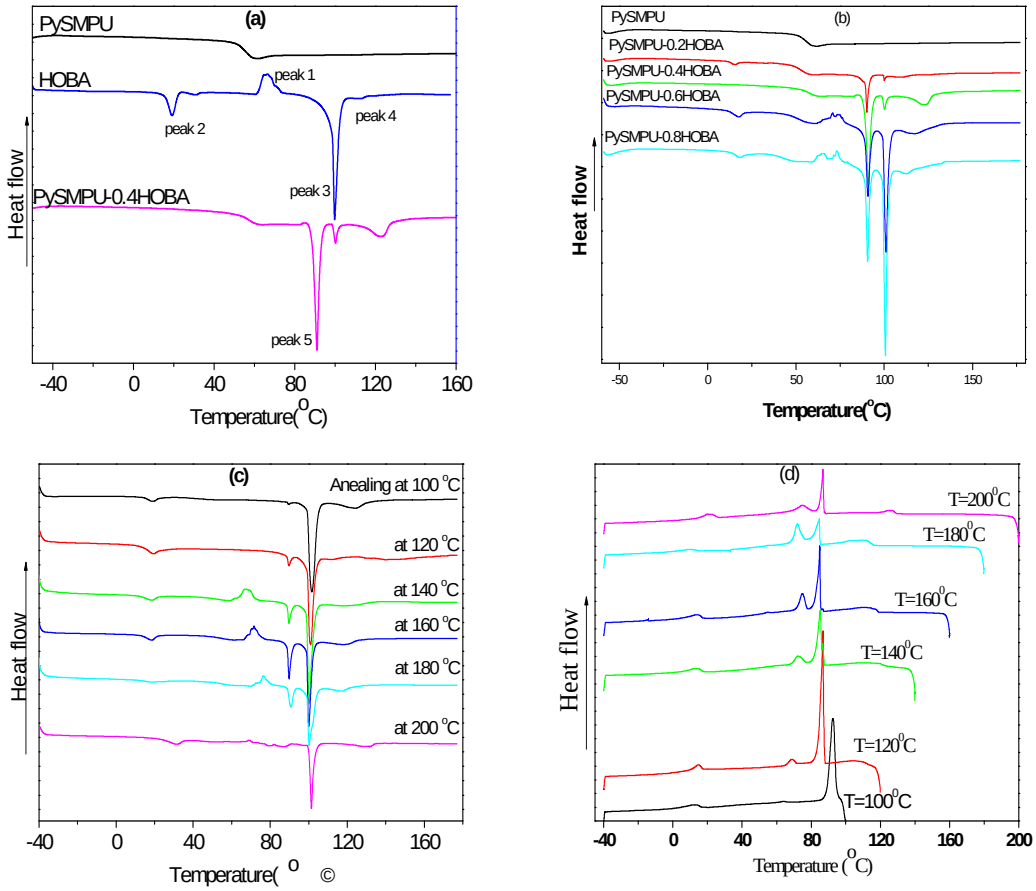

Figure 3. The second DSC heating curves for (A) PySMPU-0.4HOBA compared with pure HOBA and pure PySMPU and (B) SLCSMPU complexes with different HOBA contents, along with the second DSC heating curves (C) and the cooling DSC curves (D) for PySMPU-0.4HOBA samples treated at different temperatures

DSC was used to study the supramolecular structure and phase transitions of the SLCSMPU complex. DSC curves were recorded using a TA Instrument DSC Q200 at a heating rate of 10 °C/min. Figure 3 shows the second DSC heating curves for the SLCSMPU complexes. Figure 3(A) demonstrates that the pure PySMPU has only one glass transition at 54 °C. The pure HOBA has an exothermic peak (peak 1) at 67 °C, two obvious endothermic peaks (peak 2 and peak 3) at 18 °C and 100 °C, respectively, and a weak endothermic peak (peak 4) at 113 °C. Peak 1 represents the cold crystallisation of the HOBA since it can not be detected on the first DSC heating curves (see ESI Fig. B†). Peaks 2 and 3 are the crystal melting temperatures (T_m) for pure HOBA due to the two types of crystals that form. Peak 4 represents the phase transition from an anisotropic phase to an isotropic phase. These observations are in accordance with an earlier communication.[37] When the HOBA mesogen is tethered to the PySMPU backbone *via* hydrogen bonding to form the SLCSMPU complex, the glass transition of the PySMPU phase can be determined on the second DSC heating curve, as shown in Figure 3(A).

The cold crystallisation (peak 1) and the first type of crystal melting transition (peak 2) observed for the pure HOBA both disappear for lower HOBA contents, e.g., samples PySMPU-0.2HOBA and PySMPU-0.4HOBA, as shown in Figure 3(B). Interestingly, a new crystal melting peak (peak 5) can be detected at 91.9 °C, while the second HOBA crystal melting transition peak (peak 3) remains constant at approximately 100 °C for all of the SLCSMPU complexes. This new peak (peak 5) must be from the hydrogen-bonded HOBA mesogens because the hydrogen-bonded HOBA crystal melting transition peak appears only in the SLCSMPU complexes and gets stronger as the HOBA content increases, whereas the first type of HOBA crystal melting peak (peak 2) and cold crystallisation peak (peak 1) tend to occur with higher HOBA contents, e.g., in samples PySMPU-0.6HOBA and PySMPU-0.8HOBA, as shown in Figure 3(B). The density of the second type of HOBA crystal melting transition peak also increases with increase HOBA content. Similar to previous studies on SMPU-LC composites,[37] the free HOBA mesogen was formed when the HOBA content was higher. This suggests that SLCSMPU has a phase-separation structure composed of an amorphous PySMPU phase and a HOBA phase, including the hydrogen-bonded HOBA crystalline phase and the free HOBA crystalline phase. Thus, we can confirm that a hydrogen-bonded supramolecular liquid crystalline structure is formed in the SLCSMPU complexes. This hypothesis is further verified by the effect of heat treatment, as described below.

The influence of heat treatment was investigated systematically using DSC measurements. The PySMPU-0.6HOBA samples were selected for the heat treatment experiment. The samples were first heated to 100 °C, 120 °C, 140 °C, 160 °C, 180 °C and 200 °C. After cooling to -60 °C, the second DSC heating curve from -60 °C to 180 °C and the cooling curves were recorded for analysis, as shown in Figure 3(C-D). Figure 3(C) shows that there is no crystal melting transition peak or cold crystallisation peak between 0 and 100 °C when the treatment temperature is below 100 °C. However, the hydrogen-bonded HOBA crystal melting peak (peak 5) appears when the treatment temperature is increased to 120 °C. This peak becomes stronger as the treatment temperature increases to 160 °C and becomes weaker when the temperature exceeds 180 °C. This peak disappears above 200 °C, as shown in Figure 3(C). In contrast, the second type of HOBA crystal melting transition peak at 100 °C becomes weaker as the temperature increases from 100 °C to 160 °C and becomes stronger as the temperature increases from 160 °C to 200 °C. In the DSC cooling curves in Figure 3(D), a new crystallisation peak appears at 74 °C, which can be attributed to the hydrogen-bonded HOBA crystalline phase. This peak strengthens at annealing temperatures higher than 120 °C and weakens at annealing temperatures higher than 200 °C. Thus, we can again confirm that hydrogen-bonded HOBA is formed in the SLCSMPU complex and that heat treatment plays an important role in the formation of the hydrogen-bonded

supramolecular liquid crystalline structure.

3.3 Liquid crystalline properties

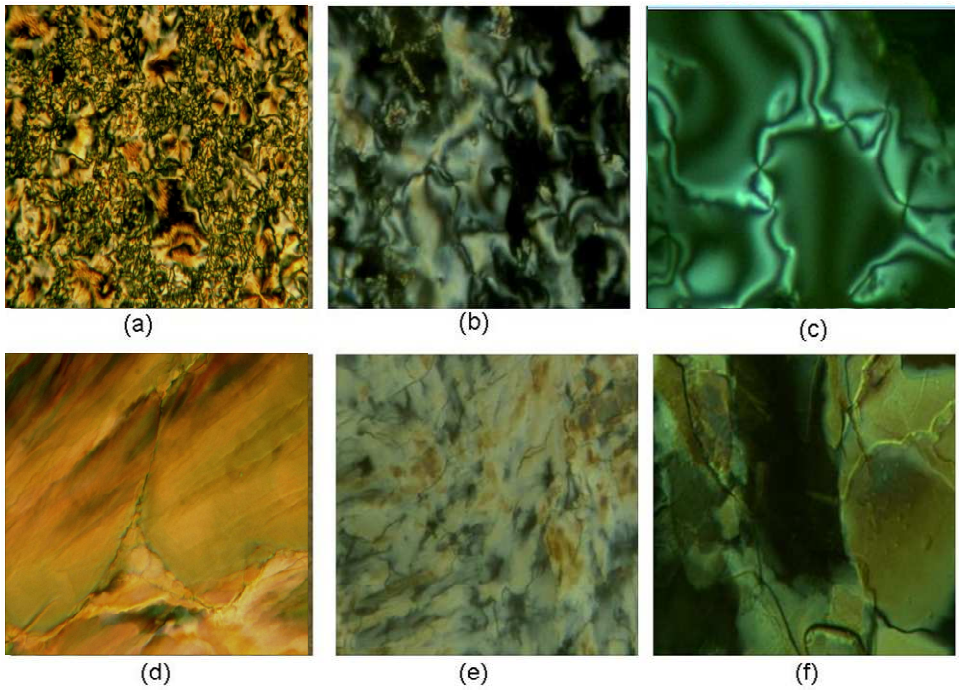

Figure 4. POM images (×400) for pure HOBA (a), PySMPU-0.4HOBA (b) and PySMPU-0.8HOBA (c) at 130 °C; POM images (×400) for pure HOBA (d), PySMPU-0.4HOBA (e) and PySMPU-0.8HOBA (f) at 25 °C

The phase transition behaviour of the SLCSMPU complexes was further investigated using the POM instrument. Figure 4 shows the POM images for pure HOBA, PySMPU-0.4HOBA and PySMPU-0.8HOBA in their liquid crystalline states (e.g., 130℃) and in their crystalline states (e.g., 25℃). The POM data show that the pure HOBA kept its crystalline state below 85℃, and the phase transition started at about 90℃. Mesomorphic phase was detected locally within the temperature range of 90℃ to 106℃ due to the crystal melting process of HOBA. This process was very consistent with the DSC observation (see ESI Fig. C†). Thereafter, HOBA entered the liquid crystalline state between temperatures of 106 ºC and 138 ºC. A schlieren texture showing only four brush singularities, which is characteristic of smectic C phase [45], was observed above 127℃. Finally, phase transition from smectic C phase to isotropic phase occurs at 138 ºC (see ESI Fig. D† and ESI Video A†). This phase transition was very consistent with the previous report that HOBA showed smectic C phase within the temperature range of 85℃ to 132.5 ºC. A typical smectic C phase is presented in Figure 4(a). Upon cooling, the pure HOBA entered the crystalline phase at temperatures lower than 84 ºC. The crystalline POM image at 25 ºC is presented in Figure 4(d). No significant texture change was observed for pure HOBA, although the DSC

curves suggested different crystal melting transitions below 84 ºC. When HOBA was incorporated into the PySMPU to form the SLCSMPU complex, similar phase transition was observed in the sample PySMPU-0.6HOBA. Below 91 ºC, crystalline phase was observed in a local region containing HOBA mesogens while the polymer matrix kept isotropic phase during the whole process. Within the temperature range of 91 ºC, to 105 ºC, part of HOBA region showed mesomorphic phase resulting from crystal melting of part of HOBA mesogen and entering the liquid crystalline phase. When the temperature was increased to about 131 ºC, the smectic C phase could also be detected below 135℃; but entered the isotropic phase above 136℃(see ESI Fig. E† and ESI Video B†). This process is also very consistent with their DSC observation (see ESI Fig. C†). The typical schlieren texture for the smectic C phase were also observed between 100 ºC and 135 ºC for both the PySMPU-0.4HOBA and PySMPU-0.8HOBA upon heating and cooling, as shown in Figure 4(b-c). This indicates that the smectic C liquid-crystalline phase remains reversible in the SLCSMPU complex. Similarly, a crystalline phase below 80 ºC can be seen in Figure 4(e-f). Compared to PySMPU-0.4HOBA, the higher HOBA content of PySMPU-0.8HOBA resulted in more obvious smectic C phase and crystalline phases because the sample contained not only the hydrogen-bonded complexes of HOBA but also the HOBA dimers, as discussed above. In contrast, samples with less HOBA formed hydrogen bonds with a small portion of the HOBA dimers. Moreover, in contrast to the previously reported hydrogen-bonded pyridine containing the mesogenic units[24], the present hydrogen-bonded HOBA retains its liquid crystalline properties. Compared with pure HOBA, the SLCSMPU complex not only maintained the intrinsic smectic C liquid-crystalline properties of the HOBA but also formed a stable polymeric film that can be used in various applications.

3.4 Morphology

The morphology of the SLCSMPU complex was investigated systematically. As mentioned above, the SLCSMPU complexes form phase-separated structures composed of an amorphous PySMPU matrix and various HOBA crystalline phases. The phase-separated structures were confirmed in the polymeric film by the POM and bright-field images acquired in reflection mode, as shown in Figure 5(a-b). Figure 5(a) shows that the polymeric film contained both an anisotropic phase and an isotropic phase at room temperature. The magnified bright-field image shows that the anisotropic phase resulted from the crystalline phase of HOBA. Additionally, some very small crystals existed in the isotropic phase, as shown in Figure 5(b). These small crystals were attributed to the hydrogen-bonded HOBA crystals. This confirms that hydrogen bonding occurs between the PySMPU and the HOBA. Additionally, the SEM images indicated two-phase separated structures, as shown in Figures 5(c) and (d). One phase represented the polyurethane matrix, while the other phase likely represented the HOBA

crystalline phase because numerous large, roughened crystals were detected, as shown in Figure 4(d). These results are consistent with the DSC and POM data.

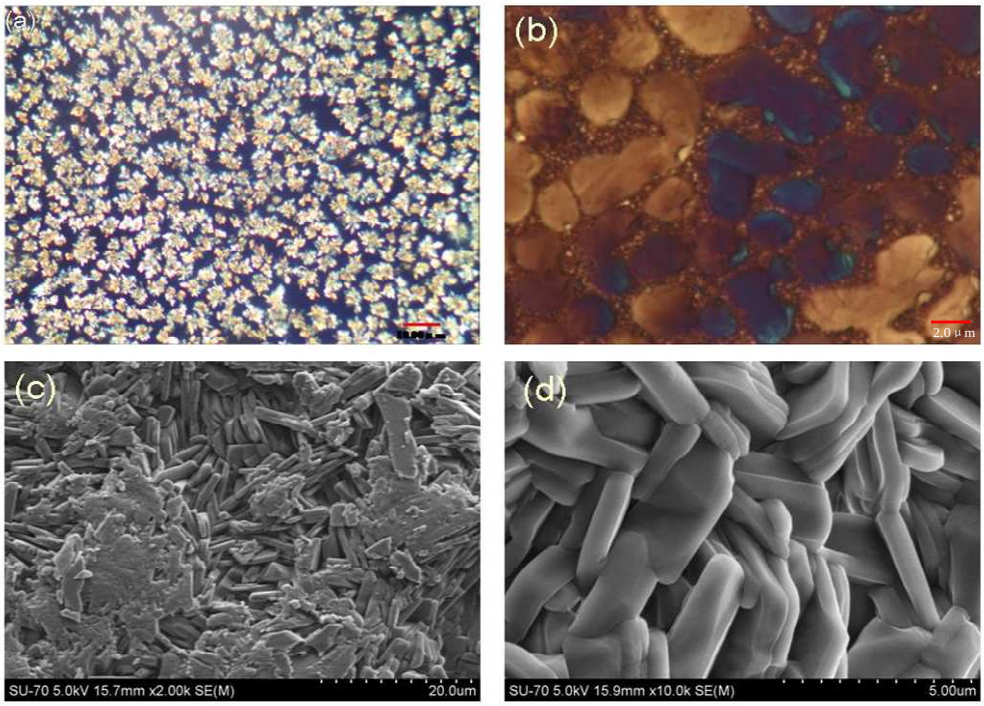

Figure 5. POM image (a) and bright-field image (b) in reflection mode for the polymeric film and SEM images (c-d) from the broken face of the PySMPU-0.8HOBA sample

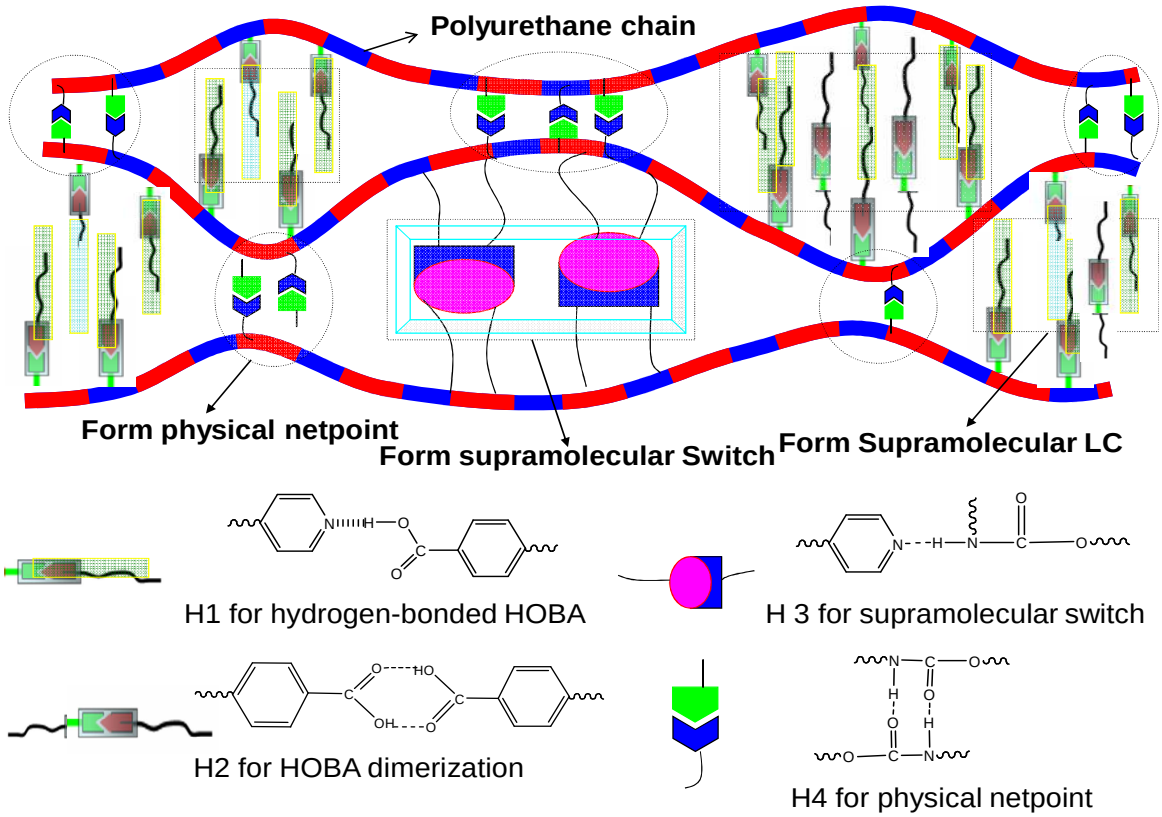

Scheme 4. Supramolecular networks of SLCSMPU complex

According to the above analysis, we can describe the supramolecular network of the SLCSMPU complex, as shown in Scheme 4. As discussed above, the polyurethane backbone is composed of BINA and HDI units. The pedant pyridine ring serves as an H-acceptor, which can form hydrogen bonds (coded as H1, see Scheme 4) with the -COOH of HOBA. This kind of hydrogen bond has also been confirmed in previous literatures [31,36]. Thus, the HOBA containing flexile tail can be stably attached to the polyurethane chain. However, as discussed above, when the molar ratio of HOBA/BINA is higher than 0.4, a lot of free HOBA molecules tends to form dimers through hydrogen bonding (coded as H2, see Scheme 4) creates a long lath-like structure with a three-ring core and two flexible terminal chains[43]. Therefore, the hydrogen-bonded and free HOBA mesogens can both congregate into the crystalline phase at room temperature and self-assemble into a liquid crystalline phase above 100 ºC. Additionally, the pedant pyridine ring also forms hydrogen-bonded supramolecular switches with the NH urethane groups (coded as H3, see Scheme 4), as discussed in the previous literature.[22, 32-35] However, this kind of hydrogen bonding may be disturbed in the SLCSMPU complex as discussed above. Temperature-dependent FT-IR spectra provide another proof to this different type of hydrogen bonding (see ESI Fig. F†). The frequency change of pyridine ring stretching vibrations versus temperature is not linear in the pure SMPU, meaning the cleavage of hydrogen bonds serving as thermal-induced molecular switch, while no significant positional change is observed in the SLCSMPU complex, implying the formation of hydrogen bonding between pyridine rings with HOBA in the SLCSMPU complex. In addition, temperature-dependent FT-IR spectra show that the N-H stretching vibration shows an abrupt increase in frequency at about 70 ℃ in both pure SMPU and SLCSMPU complex. It implies that supramolecular molecular switch still exists in the SLCSMPU complex. Comparatively, the hydrogen bonding at the position of N-H gets weaker since the N-H stretching vibration frequency shifts to higher wavenumber in the SLCSMPU complex. Finally, similar to the structures of common polyurethanes, the hydrogen bonding among urethane groups (coded as H4) can also form stable physical net points because the second cleavage of hydrogen bonding at N-H stretching vibrations tends to occur above 140℃ in the temperature-dependent FT-IR spectra(see ESI Fig. F†). Thus, the polyurethane maintains its intrinsic structure for exhibiting the shape memory effect and the HOBA maintains its intrinsic liquid crystalline properties.

3.5 Dynamic mechanical properties

Dynamic mechanical properties are very important for predicting phase transitions and shape memory effects. In this study, the pure PySMPU and the SLCSMPU complex were compared. Figure 6 shows the dependence of the storage modulus and tanδ on temperature. The pure PySMPU has two transition peaks on the tanδ curves

and three platforms on the storage modulus curves. The first transition is a β transition associated with the movement of the side chains due to dissociation of the hydrogen bonds in the pyridine ring serving as thermal-induced molecular switch. It is well-known that the storage modulus of BINA-HDI-based polyurethane is greatly influenced by the hydrogen bonding. Thus, the dissociation of the hydrogen bonds results in another significant decrease in the storage modulus during the β transition, as shown in Figure 6(a). The second transition represents the T_g transition of the amorphous phase. When the HOBA is incorporated into the PySMPU, a new transition peak appears at a higher temperature on the tanδ curves as shown in Figure 6(b). On the storage modulus curves, the modulus decreases during the β transition and T_g transition. Another modulus decrease occurs for the SLCSMPU complex at 95 ºC for PySMPU-0.2HOBA, 97 ºC for PySMPU-0.4HOBA, 98 ºC for PySMPU-0.6HOBA and 99 ºC for PySMPU-0.8HOBA, as shown in Figure 6(a). These transition temperatures are very close to the second crystal melting temperature observed on the DSC curves. Thus, this new transition can be attributed to the second crystal melting transition. As the HOBA content increases, the T_g transition peaks density becomes weaker, while the second crystal melting transition peak becomes stronger, as shown in Figure 6(b). Thus, we can confirm that two-phase separated structures composed of the polyurethane matrix and the HOBA crystals form in the SLCSMPU complexes. However, this is no significant decrease in modulus and no transition peak on the tanδ curves above 135℃, at which the smectic C phase enters into isotropic phase as discussed above. The slight modulus changing may be resulted from only small change of few percent of HOBA mesogens as shown in Figure 6. This observation indicates that there should be a small temperature dependence of the degree of association in both hydrogen-bonded HOBA and free HOBA dimers at the transition to the isotropic state. Thus, reversible smectic C phase can be achieved upon heating as well as upon cooling. Therefore, the DMA curves reveal that the modulus of the SLCSMPU complexes continuously decrease from 20 to 100 ºC due to the weak glass transition and the dissociation of the stronger intermolecular hydrogen bonds in the PySMPU matrix. An additional significant modulus decrease should be resulted from the crystal melting transition of the HOBA phase. According to the multiphase structure requirement for triple-functionality discussed above, the SLCSMPU complex tends to display an excited triple-shape functionality due to the multiple phase transition with the multi-step modulus decrease.

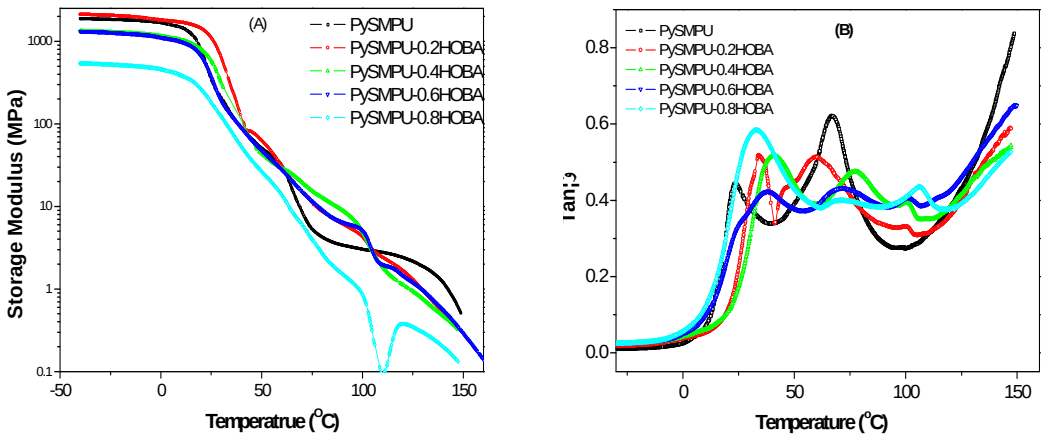

Figure 6. DMA curves for pure PySMPU (a) and the SLCSMPU-0.8HOBA complex (b)

3.6 Triple-shape functionality

A two-step programming process is usually required to achieve triple-shape functionality, where the stepwise formation of two independent shapes (A and B) occurs. In contrast, the recently developed one-step programming process facilitates triple-shape technology, substantially increasing the attractiveness of this technology for technical and medical applications. In the one-step programming process, deformed shapes are fixed below the first recovery temperature (T_{r1}) after the temporary shapes are deformed at a temperature T, which is higher than the second recovery temperature (T_{r2}) ($T>T_{r2}$). The triple shape recovery is then achieved in two stages of temperature recovery as the temperature is increased to T_{r1} and T_{r2}. We proposed another one-step programming process to achieve the triple-shape functionality. In this process, the temporary shape is also fixed below $T_{r1,}$ while the temporary shapes are deformed at relatively low temperatures T_1 ($T_{rl}<T<T_{r2}$) because higher temperatures may destroy the physical net points. The first stage of shape recovery is recorded at T_{r1}, and the second stage of shape recovery is recorded at T_{r2}. Figure 7 shows the triple-shape memory behaviours of the SLCSMPU complex with various HOBA contents for our one-step programming process. For the pure PySMPU, which has only one amorphous phase, the temporary shape is achieved at 80 ºC and is fixed at room temperature. The deformed strain is almost recovered when the temperature is increased to 80℃, with no further strain recovery above 100 ºC. That is, the pure PySMPU shows only dual-shape recovery. However, triple-shape recovery is achieved due to the phase-separating structures in the PySMPU-0.4HOBA, PySMPU-0.6HOBA, PySMPU-0.8HOBA and PySMPU-1.0HOBA samples, as shown in Figure 7 (b-e). For instance, although the strain is deformed at 80 ºC and fixed at room temperature, the PySMPU-0.6HOBA sample recovers only 65% of the deformed strain on the first stage of recovery at 80 ºC. The remaining 35% strain is recovered on the second stage of recovery at 100 ºC. This triple shape recovery process of sample PySMPU-0.6HOBA is also illustrated

with photos in supporting information (see ESI Fig. G†). In the SLCSMPU complex, triple-shape recovery becomes obvious when the molar ratio of HOBA/BINA is less than 0.8. However, the second stage strain recovery becomes very weak when the molar ratio is greater than 1.0. No strain recovery is measured in the second stage strain of recovery for the PySMPU-1.3HOBA sample, possibly because the higher HOBA content resulted in a continuous HOBA crystalline phase that may destroy the physical net points in the SLCSMPU complex required for shape recovery. Thus, the excited triple-shape functionality from the one-step programming process results from multiple phase transitions. The first stage strain recovery is associated with the glass transition of the PySMPU matrix, whereas the second stage strain recovery is greatly influenced by the crystal melting transition of the HOBA phase. The only prerequisite is that the physical net points must be well-maintained in the supramolecular liquid crystalline structure during the one-step programming process. This modified one-step programming process provides another strategy to achieve the two stage shape recovery under a relative lower deformation temperature without destroying the bulk properties of polymer or additives. It has great potential applications in smart drug control releasing, multiple stage warning system and self-healing system.

4. Conclusions

This paper describes a supramolecular liquid crystalline shape memory polyurethane (SLCSMPU) complex that exhibits both liquid crystalline and shape memory properties using HOBA incorporated into PySMPUs. FT-IR confirmed that the HOBA was tethered to the PySMPU *via* strong hydrogen bonds between the pyridine rings and the COOH of the HOBA to form the SLCSMPU complex. The DSC results showed that hydrogen-bonded supramolecular liquid crystalline structures were formed in the SLCSMPU complexes and that heat treatment played an important role in the formation of the supramolecular liquid crystalline structure. Thus, the SLCSMPU complex not only maintains the intrinsic smectic C liquid-crystalline properties of HOBA, but also forms a stable polymeric film for use in various applications in shape memory materials. Additionally, the morphological investigations showed that the SLCSMPU complex formed two-phase separated structures composed of an amorphous polyurethane matrix and a HOBA crystalline phase that included hydrogen-bonded crystalline HOBA and a free HOBA crystalline phase. Therefore, a simple one-step programming process can be used to generate SLCSMPU complexes with excited triple-shape functionalities due to their multiple phase transitions, particularly when the molar ratio of HOBA/BINA is less than 0.8.

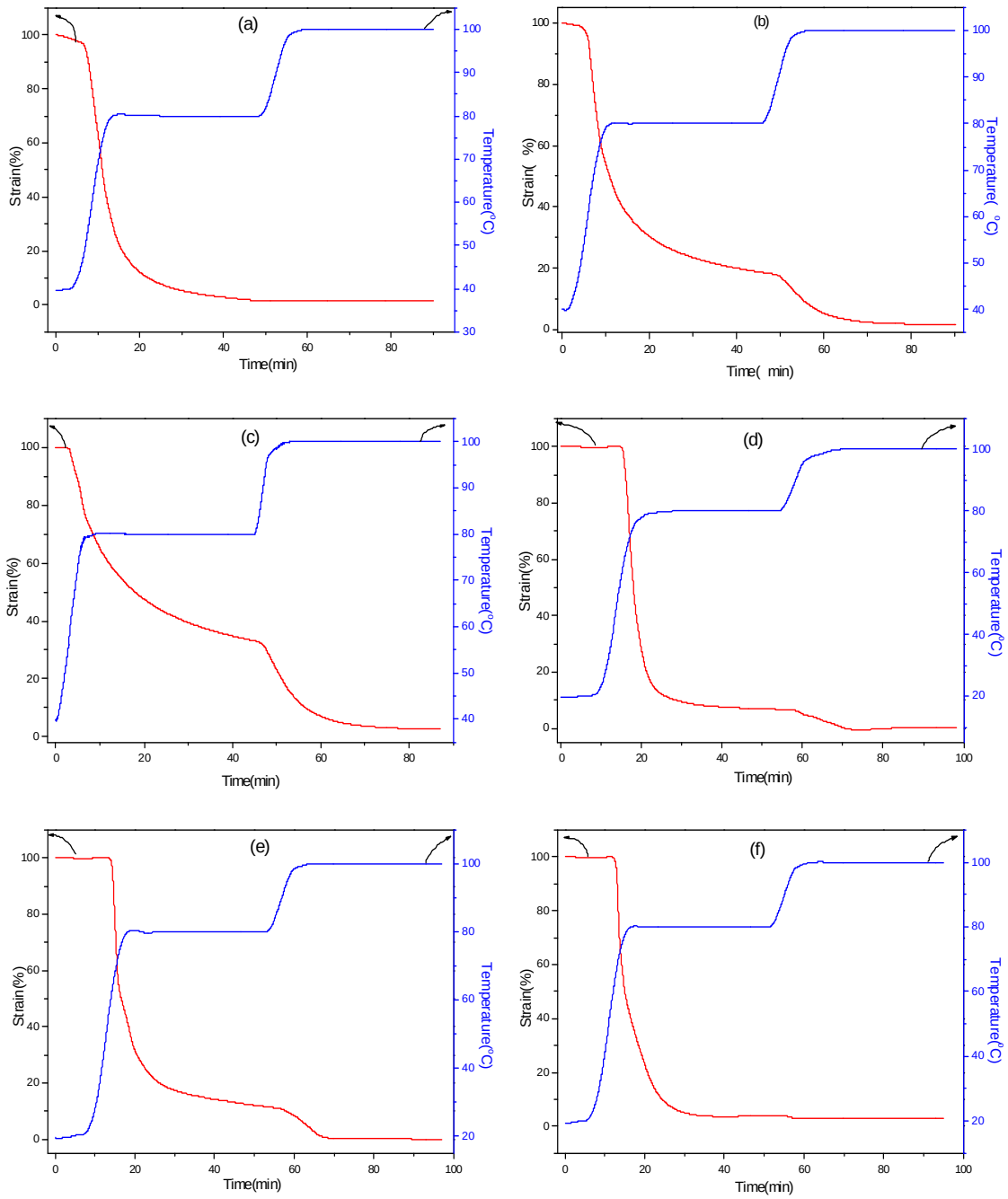

Figure 7. Triple-shape memory behaviours for the SMPU-LC composites with various HOBA contents (a-pure PySMPU; b-PySMPU-0.4HOBA; c-PySMPU-0.6HOBA; d-PySMPU-0.8HOBA; e-PySMPU-1.0HOBA; f-PySMPU-1.3HOBA)

Acknowledgements

This work was financially supported by the Natural Science Foundation of China (grant No. 21104045), the Special Research Foundation of the Shenzhen Government for Strategic Emerging Industries (grant No. JCYJ20120613102842295; GJHS20120621140852619; JCYJ20120613172439451) and the Special Research Foundation of Shenzhen Oversea High-level Talents for Innovation and Entrepreneurship (Grant No.

KQCX20120807153115869). The authors would also like to thank Prof. Jean-Marie Lehn, the Nobel Prize Laureate in 1987, and Prof. Jin-lian Hu of the Hong Kong Polytechnic University for their guidance.

References

1. J. L. Hu and S. J. Chen, *J.Mater.Chem.*, 2010, **20**, 3346-3355.
2. H. Meng and G. Li, *Polymer*, 2013, **54**, 2199-2221.
3. K. S. S. Kumar, R. Biju and C. P. R. Nair, *React. Funct. Polym.*, 2012,**73**, 421-430.
4. Y. Niu, P. Zhang, J. Zhang, L. Xiao, K. Yang and Y. Wang, *Polym. Chem.*,2013, **3**, 2508-2516.
5. Y. Han, T. Bai, Y. Liu, X. Zhai and W. Liu, *Macromol.Rapid Comm.*, 2011, **33**, 225-231.
6. T. Ware, K. Hearon, A. Lonnecker, K. L. Wooley, D. J. Maitland and W. Voit, *Macromolecules*, 2012, **45**, 1062-1069.
7. M. Bothe, K. Y. Mya, E. M. J. Lin, C. C. Yeo, X. Lu, C. He and T. Pretsch, *Soft Matter*, 2012, **8**, 965-972.
8. J. M. Cuevas, R. Rubio, L. German, J. M. Laza, J. L. Vilas, M. Rodriguez and L. M. Leon, *Soft Matter*, 2012, **8**, 4928-4935.
9. J. Zhang, Y. Niu, C. Huang, L. Xiao, Z. Chen, K. Yang and Y. Wang, *Polym. Chem.*, 2012, **3**, 1390-1393.
10. T. Xie, *Nature*, 2010, **464**, 267-270.
11. H.-J. Radusch, I. Kolesov, U. Gohs and G. Heinrich, *Macromol. Mater. Eng.*, 2012, **297**, 1225-1234.
12. Q. Zhao, M. Behl and A. Lendlein, *Soft Matter*, 2012, **9**, 1744-1755.
13. M. Behl and A. Lendlein, *J.Mater.Chem.*, 2010, **20**, 3335-3345.
14. X. Luo and P. T. Mather, *Adv. Funct.Mater.*, 2010, **20**, 2649-2656.
15. H. Meng and G. Li, *Polymer*, 2013, **54**, 2199-2221.
16. M. Behl, I. Bellin, S. Kelch, W. Wagermaier and A. Lendlein, *Adv. Funct.Mater.* 2009, **19**, 102-108.
17. J. R. Kumpfer and S. J. Rowan, *J. Am. Chem.Soc.*, 2011, **133**, 12866-12874.
18. S. J. Chen, J. L. Hu, S. G. Chen and C. L. Zhang, *Smart Mater.Struct.*, 2011, **20**, 06500301-06500309.
19. S. Zhang, Z. J. Yu, T. Govender, H. Y. Luo and B. J. Li, *Polymer*, 2008, **49**, 3205-3210.
20. J.M. Lehn, *Aust. J.Chem.*, 2010, **63**, 611-623.
21. M.M. Fan, Z.J. Yu, H.-Y. Luo, Z. Sheng and B.-j. Li, *Macromol.Rapid Comm.*, 2009, **30**, 897-903.
22. S. Chen, J. Hu, C.W. M. Yuen and L. Chan, *Mater. Lett.*, 2009, **63**, 1462-1464.
23. Z.Q. Dong, Y. Cao, Q.J. Yuan, Y.F. Wang, J.H. Li, B.J. Li and S. Zhang, *Macromol. Rapid Comm.*, 2013, **34**, 867-872.

24. H. Chen, Y. Liu, T. Gong, L. Wang, K. Zhao and S. Zhou, *RSC Adv.*, 2013, **3**, 7048-7056.
25. D. Chen, L. Wan, J. Fang, X. Yu and M., *Polym. Bull.*, 2002, **0**, 5-18.
26. M. R. Hammond and R. Mezzenga, *Soft Matter*, 2008, **4**, 952-961.
27. T. Kato, Y. Kubota, M. Nakano and T. Uryu, *Chem. Lett.*, 1995, 1127-1128.
28. T. Kato, M. Fukumasa and J. M. J. Frechet, *Chem. Mater.*, 1995, **7**, 368-372.
29. W. H. Binder and R. Zirbs, in *Hydrogen Bonded Polymers*, 2007, 207, 1-78.
30. T. Kato and J. M. J. Frechet, *Macromol.Symp.*, 1995, **98**, 311-326.
31. G. Ambrozic and M. Zigon, *Polym. Int.*, 2005, **54**, 606-613.
32. S. Chen, J. Hu, H. Zhuo, C. M. Yuen and L. Chan, *Polymer*, 2010, **51**, 240-248.
33. S. Chen, J. Hu, C.W. M. Yuen and L. Chan, *Polymer*, 2009, **50**, 4424-4428.
34. S. Chen, J. Hu and S. Chen, *Polym. Int.*, 2012, **61**, 314-320.
35. S. Chen, J. Hu and H. Zhuo, *J.Mater. Sci.*, 2011, **46**, 6581-6588.
36. G. Ambrozic, J. Mavri and M. Zigon, *Macromol. Chem. Phys.*, 2002, **203**, 439-447.
37. S. Chen, H. Yuan, Z. Ge, S. Chen, H. Zhuo and J. Liu, *J.Mater.Chem. C*, 2014, **2**, 1041-1049.
38. S. J. Chen, J. L. Hu, S. G. Chen and C. L. Zhang, *Smart Mater. Struct.*, 2011, **20**, 06500301-06500309.
39. R. M. Kasi, S. K. Ahn and P. Deshmukh, *Macromolecules*, 2010, **43**, 7330-7340.
40. S. Chen, J. Hu, C.-W. M. Yuen and L. Chan, *Polym. Int.*, 2010, **59**, 529-538.
41. P. Wu, G. J. Deng, S. L. Xu, Q. H. Fan, L. J. Wan, C. Wang and C. L. Bai, *Chinese Sci. Bull.*, 2002, **47**, 1514-1517.
42. Z.Sideratou, D.Tsiourvas, C.M.Paleos and A.Skoulios, *Liq.Cryst.* 1997, **22**, 51-60.
43. R. I. Nessim and M. I. Nessim, *Thermalchim. Acta*, 2010, **511**, 27-31.
44. M.M.Naoum, A.A.Fahmi and H.A.Ahmed, *Liq.Cryst.* 2012, **562**, 43-65.
45. I.Nishiyama, T.Yamamoto, J.Yamamoto, J.W.Goodby and H.Yokoyama, *J. Mater. Chem.*, 2003, **13**, 1868-1876

Development of Supramolecular Liquid-Crystalline Polyurethane Complexes Exhibiting Triple-shape Functionality Using a One-step Programming Process

Shaojun Chen[1], Hongming Yuan[1], Shiguo Chen[1], Haipeng Yang, Zaochuan Ge[1]*[a)],

Haitao Zhuo[2]*[b)], Jianhong Liu[2],

[1]*Shenzhen Key Laboratory of Special Functional Materials, College of Materials Science and Engineering, Shenzhen University, Shenzhen,518060, China.* [2]*Shenzhen Key Laboratory of Functional Polymer, College of Chemistry and Chemical Engineering, Shenzhen University, Shenzhen, 518060, China.*

*Corresponding author: College of Materials Science and Engineering，Shenzhen University, Shenzhen 518060, China. Tel and Fax: +86-755-26534562. E-mail: [a)]Z.C.Ge gezc@szu.edu.cn; [b)]H.T.Zhuo haitaozhuo@163.com

Graphic abstract

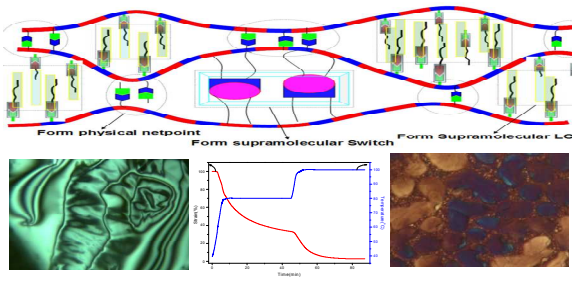

Supramolecular shape memory liquid crystalline polyurethanes showing smectic C properties and exhibiting triple-shape functionality using one-step programming process are prepared.